Ab Initio EPR Study of S_3^- and Se_3^- Defects in Alkali Halides

F. STEVENS,[1,2] H. VRIELINCK,[1] F. CALLENS,[1] E. PAUWELS,[2] V. VAN SPEYBROECK,[2] M. WAROQUIER[2]

[1]*Ghent University, Department of Solid State Sciences, Krijgslaan 281-S1, B-9000 Ghent, Belgium*

[2]*Ghent University, Laboratory of Theoretical Physics, Proeftuinstraat 86, B-9000 Ghent, Belgium*

Received 7 September 2003; accepted 27 August 2004
Published online 6 December 2004 in Wiley InterScience (www.interscience.wiley.com).
DOI 10.1002/qua.20389

ABSTRACT: Calculations using density functional theory are performed to study the electron paramagnetic resonance (EPR) and electron nuclear double resonance (ENDOR) properties of S_3^- and Se_3^- impurities in alkali halide lattices. Cluster in vacuo models are used to describe the defect and the lattice surroundings. The trivacancy defect model proposed in the literature is able to reproduce both the experimental principal values and directions of the g tensor for S_3^- and Se_3^- defects doped in alkali halides. The alternative monovacancy model gives rise to important discrepancies with experiment and can be discarded. For the KCl lattice, the hyperfine tensors of the S_3^- and Se_3^- molecular ions also agree well with the available experimental data, giving further evidence to the trivacancy model. In addition, for NaCl:S_3^- and KCl:S_3^- computational results for the ^{23}Na and ^{35}Cl superhyperfine and quadrupole tensors are compared with experimental ENDOR parameters. Int J Quantum Chem 102: 409–414, 2005

Key words: density functional theory (DFT); electron paramagnetic resonance (EPR); electron nuclear double resonance (ENDOR); ionic lattice; chalcogen defect; trivacancy model

Introduction

Sulfur and selenium doping in alkali halides and subsequent exposure to ionizing radiation gives rise to a wealth of paramagnetic defects. With the aid of electron paramagnetic resonance (EPR) and electron nuclear double resonance (ENDOR) mono- [1–4], di- [5–7], tri- [8–10], and tetra-atomic [8] centers have been identified. Despite the accuracy of the experiments and the analyses of these data, our knowledge about the structure of these defects is still incomplete. Recently, cluster in vacuo density functional theory (DFT) calculations [11, 12] for S_2^-, SSe^- and Se_2^- molecular ions have shown that the ground state, the g and hyperfine tensor may be satisfactorily reproduced in nine alkali ha-

Correspondence to: F. Callens; e-mail: freddy.callens@UGent.be

This article was presented at the 10th International Conference on the Applications of Density Functional Theory in Chemistry and Physics, September 7–12, 2003, Brussels, Belgium.

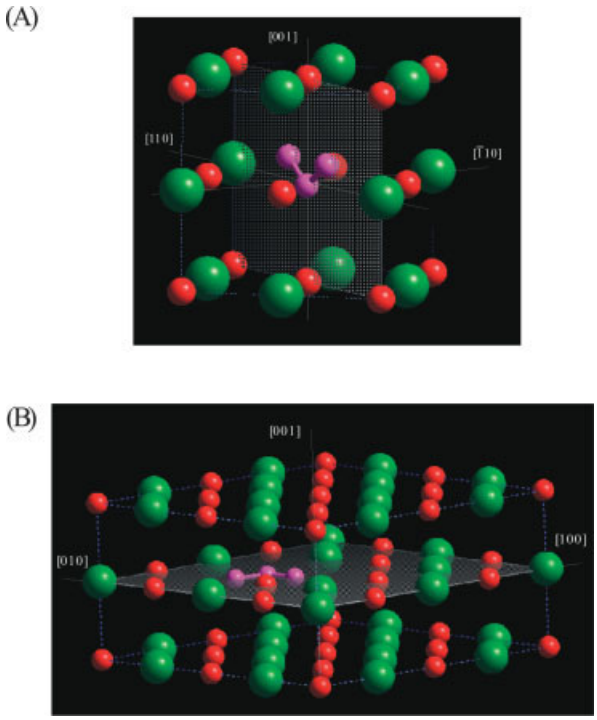

FIGURE 1. Mono- (A) and trivacancy (B) structure for the S_3^- defect. The alkali and halide atoms are colored red and green, respectively.

lide (MZ, M = Na, K, Rb and Z = Cl, Br, I) host lattices. This opens favorable perspectives to solve at least some of the remaining problems concerning sulfur and selenium defects in these lattices, such as their precise structure or ground-state properties.

The present work deals with X_3^- (X = S, Se) molecular ions in alkali halides which give rise to orthorhombic centers with S = 1/2 and principal g tensor axes along [110], [$\bar{1}$10], and [001]. Two microscopic models are compatible with this symmetry: (i) a monovacancy model in which X_3^- replaces a single Z^- halide ion [Fig. 1(A)] and (ii) a trivacancy model [Fig. 1(B)] in which the paramagnetic ion replaces an $(ZMZ)^-$ unit.

Based on the theory of Walsh [13], which is developed for X_3^- ions in vacuo, some preliminary conclusions about the electronic configuration of the molecular ion in the crystal lattice can be made. According to this theory, the X_3^- ion in vacuo has a bent structure with C_{2v} symmetry and a $^2B_1$ ground state. Within the linear combination of atomic orbitals scheme, the unpaired electron resides in a molecular orbital of the following form:

$$|b_1\rangle = c_1|p_x^X\rangle + c_2\frac{|p_x^{X_1}\rangle + |p_x^{X_2}\rangle}{\sqrt{2}}, \qquad (1)$$

with the x axis perpendicular to the molecular plane X_1 and X_2 the two outer equivalent S or Se atoms and X in the center. Using Stone's formula [14, 15], the largest principal g value is found along the axis connecting the outer X atoms, which is defined as the y axis. The smallest g value is expected along the axis perpendicular to the molecular plane (x axis), and the direction of the intermediate g value corresponds with the C_2 axis of the X_3^- ion, defined as the z axis. Assuming that this theory is still valid for X_3^- ions in an ionic lattice environment, one would expect that the smallest g shift is to be found along an ⟨110⟩ direction for the monovacancy model [Fig. 1(A)] and along an ⟨001⟩ direction for the trivacancy model [Fig. 1(B)]. On these grounds, the latter model was proposed for the MZ:X_3^- defects. Nonetheless, no symmetry arguments are present to exclude the monovacancy model.

The purpose of the present cluster in vacuo DFT calculations is twofold. First, using both the mono- and the trivacancy model, we want to verify if the unpaired electron lobe and the direction of the smallest g shift are found perpendicular to the X_3^- plane for both defect structures. This would imply that the monovacancy model could be excluded. Second, it is tested to what extent the calculations are able to reproduce the EPR and ENDOR parameters of the S_3^- and Se_3^- defects in alkali halides. The main quantities determined in EPR and ENDOR experiments are the g, (super)hyperfine, and quadrupole tensors, which describe the interaction between (i) the electron spin and the external magnetic field, (ii) a nuclear spin and the electron spin,

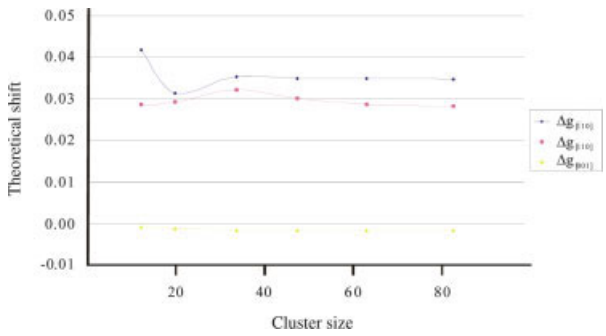

FIGURE 2. Calculated g shifts (in ppt) as a function of increasing cluster size for the NaCl:S_3^- defect structure.

TABLE I

Theoretical Δg values (in ppt) using the mono- and the trivacancy model for the NaCl:S_3^- structure, compared with experimental data.

	Experiment[a]		Theory: monovacancy		Theory: trivacancy	
	Value	Direction	Value	Direction	Value	Direction
Δg_x	−0.9	[001]	0.06	[$\bar{1}$10]	−1.6	[001]
Δg_y	44.2	[$\bar{1}$10]	37.6	[110]	34.6	[$\bar{1}$10]
Δg_z	28.5	[110]	27.1	[001]	28.1	[110]

[a] Ref. [8].

and (iii) the electric quadrupole moment of the nucleus and electric field gradients respectively. For a detailed discussion on EPR and ENDOR properties, we refer to specialized standard works [16].

Computational Details

The monovacancy model was simulated using an 89-atom cluster as described in Refs. [11, 12]. For the trivacancy model, a cluster composed of 140 atoms was used to optimize the structure of the X_3^- molecular ions. For this cluster size, EPR calculations turned out to be computationally unfeasible. Therefore, an 84-atom cluster was cut from the optimized structure (see below). Geometry optimizations were performed with the ADF1999 (Amsterdam Density Functional) program package [17–19] with basis set IV [20] and the VWN functional [21]. For both the mono- and trivacancy model, the central X_3^- ion and the nearest shell alkali atoms were treated unfrozen; for all other atoms a frozen core approximation was applied. In both defect models, the first alkali and halide lattice shells were allowed to relax while all other atoms were kept fixed at their lattice positions. The ADF program was also selected to calculate the g [22] and Q tensors [23] for both defect models, again using the VWN functional in combination with basis set IV. Using this approach, very accurate g and Q values for diatomic chalcogen defects were obtained [11, 12] but substantial discrepancies with experimental (super)-hyperfine data were observed. For this reason, a hybrid functional shall be used for calculating the (super)hyperfine values, as they produce more reliable results for these properties [24]. The frozen core approximation was applied in accordance with the computational protocol of the geometry optimizations. The (super)hyperfine tensors were calculated for the optimized ADF geometries with Gaussian98 software [25]. The B3LYP functional [21, 26–28] was used in combination with a 6-31G** basis set for the lattice environment and a 6-311++G** basis set for the X_3^- ion. For the Rb atoms, the full-electron Sadlej pVTZ basis set was applied [29].

Computational Results

VALIDATION OF THE CLUSTER SIZE FOR THE TRIVACANCY MODEL

Although geometry optimizations are feasible for a cluster composed of 140 atoms at the ADF VWN/IV level of theory, the program fails in evaluating the corresponding relevant EPR parameters. These computational limitations necessitate a reduction of the 140-atom cluster. This should be performed with great care and it should be verified that convergence of the EPR parameters under interest still takes place. To accomplish this, the cluster size dependence of the g tensor has been investigated for the S_3^- defect in NaCl. The results are displayed in Figure 2, and we may assume that sufficient convergence has been reached at least in the 84-atom cluster. This cluster fulfills the requirements of a low total charge (−4) and an accurate description of the lattice environment of the central molecular ion to limit boundary effects.

g TENSOR

Monovacancy vs. Trivacancy Model for NaCl:S_3^-

Table I reports the calculated g shifts ($\Delta g_i = g_i - g_e$; $i = x, y, z$; in ppt) for the NaCl:S_3^- defect structure using the mono- and the trivacancy model.

TABLE II

Comparison of calculated Δg values (in ppt) with the experimental ones for the S_3^- ion and the Se_3^- ion using the trivacancy model.

		Experiment			Theory		
X_3^-	Lattice	Δg_x	Δg_y	Δg_z	Δg_x	Δg_y	Δg_z
S_3^-	NaCl[a]	−0.9	44.2	28.5	−1.6	34.6	28.1
S_3^-	NaBr[a]	0.7	47.7	32.5	0.5	51.1	44.9
S_3^-	KCl[a]	0.3	47.6	29.6	1.3	40.6	30.8
S_3^-	KBr[a]	1.7	48.5	30.4	2.6	45.9	36.4
S_3^-	RbCl[b]	0.1	51.4	36.1	0.8	45.6	33.9
Se_3^-	KCl[a]	−13.8	218.2	152.2	−17.0	186.6	136.3

[a] Ref. [8].
[b] Ref. [10].

For both defect structures, the smallest g shift is found along the direction perpendicular to the molecular plane. This corresponds to a $\langle \bar{1}10 \rangle$ direction in the mono- and to a $\langle 001 \rangle$ direction in the trivacancy model. Also, the largest g shift is found along the direction of the outer two S atoms, while the intermediate g value is found along the C_2 symmetry axis for both defect models. This is in agreement with Walsh's theory [13]. The magnitude of the g shifts is nearly independent of the lattice environment. Indeed, for both defect models, the smallest g shift is close to zero, the intermediate g shift is about 28 ppt, while the largest g shift is 36 ppt on average. Therefore, no final assignment of the defect model can be made, solely based on the magnitude of the g shifts.

From a single crystal study [8], the smallest g value was found along the $\langle 001 \rangle$ direction. Hence, a trivacancy model is supported while the monovacancy model is excluded. For the trivacancy model, the computed ground-state wave function of the unpaired electron is of the form of Eq. (1) with $c_1 = 0.84$ and $c_2 = 0.54$.

In conclusion, the trivacancy model is found the reproduce in a correct way the experimental g values, and its results coincide with those predicted by the theory of Walsh.

g Tensor for MZ:X_3^-

Because the experimental g tensors of the S_3^- ion doped in NaBr, KCl, KBr, and RbCl have the same symmetry and orientation as for the NaCl lattice, we may assume that the trivacancy model is correct for all these lattices. Theoretical and experimental Δg values are listed in Table II. In all cases good agreement with the experimental g shifts is obtained.

For the Se_3^- ion doped in KCl, larger g shifts are observed both experimentally and theoretically. The quantitative agreement is fairly well.

(SUPER)HYPERFINE AND QUADRUPOLE DATA

The principal axes of the hyperfine tensor for the central sulfur or selenium nuclei, are parallel of those of the g tensor. In contrast, two principal axes of the hyperfine tensor for the two outer nuclei are expected to be tilted away from the g-tensor axes in the plane of the molecular ion by an angle $\alpha_{A,I}$.

TABLE III

Comparison of predicted and experimental hyperfine values (in MHz) for the ^{33}S and ^{77}Se interaction for KCl:S_3^- and KCl:Se_3^-.

	S_3^-		Se_3^-	
	Exp.[a]	Theory	Exp.[a]	Theory
A_x	150	148	694	632
A_y	<30	−32	135	−231
A_z	<30	−33	166	−245
$A_{x,1}$	54	40	203	225
$A_{y,1}$	n.a.	−8	0	−9
$A_{z,1}$	n.a.	−11	48	−32
$\alpha_{A,1}$	n.a.	37	20	6

[a] Ref. [9].
"A_i" ($i = x, y, z$) stands for the interaction with the central nucleus; "$A_{i,1}$" stands for the interaction with the two equivalent outer nuclei. The tilting angle $\alpha_{A,1}$ is given in degrees.

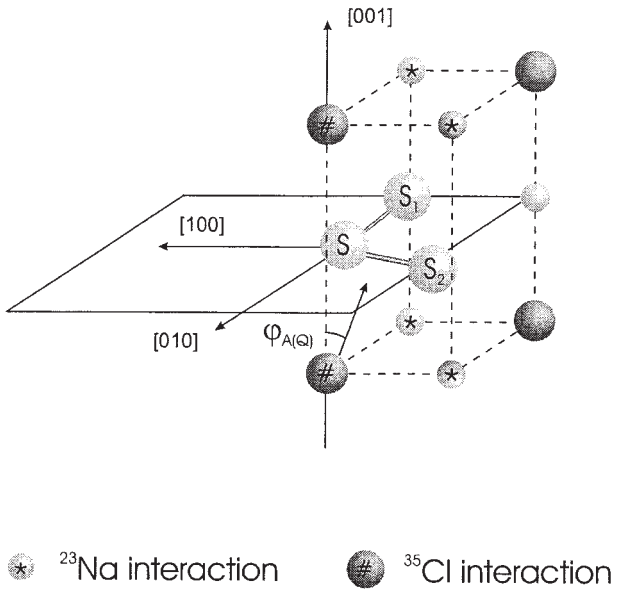

FIGURE 3. Trivacancy model for $MZ:X_3^-$, indicating the nuclei with which the interaction has been identified in the ENDOR spectra.

Experimentally, it is observed that the direction of the largest hyperfine value corresponds to the direction of the smallest g shift (g_x axis, [001]). This is perfectly reproduced by the calculations as seen in Table III. Both the ^{33}S and ^{77}Se interaction are calculated in very accurate agreement with the experimental data for KCl.

For $NaCl:S_3^-$, superhyperfine and quadrupole interactions with four equivalent sodium neighbors (Fig. 3) could be resolved using ENDOR [9]. For comparison with literature, all three principal values and three direction cosines for each principal direction are given in Table IV, and it is seen that the theoretical data are close to the experimental data. The values for the ^{23}Na quadrupole interaction are also reasonably well reproduced.

Besides the interaction with four equivalent sodium atoms, interaction with two equivalent chlorine neighbors was also identified. The ^{35}Cl superhyperfine and quadrupole interactions have axial symmetry and the principal axes are close to the g tensor axes but slightly tilted by an angle $\varphi_{A(Q)}$ in the $(1\bar{1}0)$ plane (Fig. 3). Experimental and computational data are also available for $KCl:S_3^-$, and for both crystals the same conclusions can be made (Table V): the anisotropic couplings are seriously overestimated and the quadrupole couplings are underestimated. On the other hand, isotropic cou-

TABLE V

Theoretical and experimental ENDOR data for the ^{35}Cl interaction for S_3^- in NaCl and KCl.

	NaCl		KCl	
	Exp.[a]	Theory	Exp.[a]	Theory
T_x	2.10	19.80	2.64	10.44
T_y	−1.05	−9.90	−1.32	−5.22
T_z	−1.05	−9.90	−1.32	−5.22
A_{iso}	9.96	14.90	3.94	4.93
φ_A	5.00	2.60	7.00	1.70
Q_x	0.66	0.46	0.54	0.14
Q_y	−0.33	−0.23	−0.27	−0.07
Q_z	−0.33	−0.23	−0.27	−0.07
φ_Q	n.a.	8.64	n.a.	18.60

[a] Ref. [9].
A_{iso} and T_i are equally defined as in Table IV. The tilting angle $\varphi_{A(Q)}$ is given in degrees.

TABLE IV

Theoretical and experimental ENDOR data for the ^{23}Na interaction for $NaCl:S_3^-$.

		Direction cos.				Direction cos.		
	Exp.[a]	g_x	g_y	g_z	Theory	g_x	g_y	g_z
T_x	1.72	0.986	0.075	0.147	1.62	0.980	0.086	0.179
T_y	−0.72	−0.164	−0.883	0.440	−0.65	−0.196	−0.799	0.569
T_z	−1.00	−0.164	0.440	0.883	−0.97	0.033	0.575	0.818
A_{iso}	6.48				5.14			
Q_x	−0.18	n.a.	n.a.	n.a.	−0.14	−0.933	0.248	0.262
Q_y	0.02	n.a.	n.a.	n.a.	0.06	0.326	0.882	0.324
Q_z	0.16	n.a.	n.a.	n.a.	0.08	0.152	−0.387	0.909

[a] Ref. [9].
A_{iso} stands for the isotropic part, while T_i ($i = x, y, z$) represent the anisotropic part of the A tensor.

plings and tilting angles φ_A are reproduced reasonably well. Although the agreement between experimental and theoretical ENDOR data is not in all cases satisfactory, the calculations are able to reproduce that the largest A and Q value is found close to the [001] axis, i.e., the direction of the smallest g shift.

Conclusions

In the present DFT study, the calculated magnetic resonance parameters of the S_3^- and Se_3^- molecular ions were compared with results of EPR and ENDOR single crystal measurements. A first major success of the present work is the confirmation of the $^2B_1$ ground state and the trivacancy model for X_3^- ions. The calculations clearly show that the use of the monovacancy model gives deviating results. Furthermore, both experimentally and theoretically, the directions of the smallest g shift and the largest hyperfine value, i.e., [001] axis, were found to coincide. Also, the calculations were able to reproduce the experimental g values for X_3^- ions embedded in various alkali halides.

ACKNOWLEDGMENT

The authors would like to thank the Fund for Scientific Research (FWO-Flanders, Belgium) and the Research board of Ghent University for financial support.

References

1. Hausmann, A. Zeitschrift für physik 1996, 192, 313.
2. Vannotti, E.; Morton, J. R. Phys Rev 1968, 174(2), 448.
3. Matthys, P.; Callens, F.; Boesman, E. Solid State Commun 1983, 45(1), 1.
4. Callens, F.; Matthys, P.; Boesman, E. Phys Status Solidi 1983, 118, K35.
5. Vannotti, L. E.; Morton, J. R. Phys Rev 1967, 161, 282.
6. Matthys, P.; Callens, F.; Boesman, E. Solid State Commun 1983, 45, 1.
7. Maes, F.; Callens, F.; Matthys, P.; Boesman, E. Phys Status Solidi 1990, B 161, K1.
8. Schneider, J.; Dischler, B.; Räuber, A. Phys Status Solidi 1966, 13, 141.
9. Suwalski, J.; Seidel, H. Phys Status Solidi 1966, 13, 159.
10. Maes, F.; Callens, F.; Matthys, P.; Boesman, E. Radiat Eff Defects Solids 1991, 116, 283.
11. Stevens, F.; Vrielinck, H.; Callens, F.; Pauwels, E.; Waroquier, M. Phys Rev B 2002, 66, 134103.
12. Stevens, F.; Vrielinck, H.; Callens, F.; Pauwels, E.; Waroquier, M. Phys Rev B 2003, 67, 104429.
13. Walsh, A. D. J Chem Soc 1953, 1, 2260.
14. Stone, A. J. Proc Roy Soc A 1963, 271, 424.
15. Schlick, S. J Chem Phys 1979, 70, 277.
16. Atherton, N. M. Principals of Electron Spin Resonance; Prentice Hall: New York, 1993.
17. ADF, http://tc.chem.vu.nl/SCM., Department of Theoretical Chemistry, Vrije Universiteit, Amsterdam.
18. Baerends, E. J.; Ellis, D. E.; Ros, P. Chem Phys 1973, 2, 41.
19. Guerra, F.; Visser, O.; Snijders, J. G.; te Velde, G.; Baerends, E. J. In Methods and Techniques in Computational Chemistry: METECC-95; Clementi, E.; Corongiu, G., Eds.; STEF: Cagliari, 1995, pp 305–395.
20. All standard ADF basis sets are available on the net at http://www.scm.com/Doc/atomidata.
21. Vosko, S. H.; Wilk, L.; Nusair, M. Can J Phys 1980, 58, 1200.
22. van Lenthe, E.; Wormer, P.; van der Avoird, A. J Chem Phys 1997, 107(7), 2488.
23. van Lenthe, E.; van der Avoird, A.; Wormer, P. J Chem Phys 1997, 108(12), 4783.
24. Stevens, F.; Van Speybroeck, V.; Pauwels, E.; Vrielinck, H.; Callens, F.; Waroquier, M. Phys Chem Chem Phys, accepted for publication.
25. Frisch, M. J.; Trucks, G. W.; Schlegel, H. B.; Scuseria, G. E.; Robb, M. A.; Cheeseman, J. R.; Zakrzewski, V. G.; Montgomery, Jr., J. A.; Stratmann, R. E.; Burant, J. C.; Dapprich, S.; Millam, J. M.; Daniels, A. D.; Kudin, K. N.; Strain, M. C.; Farkas, O.; Tomasi, J.; Barone, V.; Cossi, M.; Cammi, R.; Mennucci, B.; Pomelli, C.; Adamo, C.; Clifford, S.; Ochterski, J.; Petersson, G. A.; Ayala, P. Y.; Cui, Q.; Morokuma, K.; Malick, D. K.; Rabuck, A. D.; Raghavachari, K.; Foresman, J. B.; Cioslowski, J.; Ortiz, J. V.; Baboul, A. G.; Stefanov, B. B.; Liu, G.; Liashenko, A.; Piskorz, P.; Komaromi, I.; Gomperts, R.; Martin, R. L.; Fox, D. J.; Keith, T.; Al-Laham, M. A.; Peng, C. Y.; Nanayakkara, A.; Gonzalez, C.; Challacombe, M.; Gill, P. M. W.; Johnson, B.; Chen, W.; Wong, M. W.; Andres, J. L.; Gonzalez, C.; Head-Gordon, M.; Replogle, E. S.; Pople, J. A. Gaussian 98, Revision A.7; Gaussian, Inc.: Pittsburgh, PA, 1998.
26. Becke, A. D. J Chem Phys 1993, 98, 5648.
27. Lee, C.; Yang, W.; Parr, R. G. Phys Rev B 1988, 37, 758.
28. Stephens, P. J.; Devlin, F. J.; Chabalowski, F. J.; Frisch, M. J. J Phys Chem 1994, 98, 11623.
29. Basis sets were obtained from the Extensible Computational Chemistry Environment Basis Set Database, Version 6/19/03, as developed and distributed by the Molecular Science Computing Facility, Environmental and Molecular Sciences Laboratory, which is part of the Pacific Northwest Laboratory, P.O. Box 999, Richland, WA 99352, USA, and funded by the U.S. Department of Energy. The Pacific Northwest Laboratory is a multiprogram laboratory operated by Battelle Memorial Institute for the U.S. Department of Energy under contract DE-AC06-76RLO 1830. Contact David Feller or Karen Schuchardt for further information.